

## Optical double-resonance cooled-atom spectroscopy

T. Loftus, J. R. Bochinski, and T. W. Mossberg

Oregon Center for Optics and Department of Physics, University of Oregon, Eugene, Oregon 97403

(Received 15 August 2000; published 4 January 2001)

We demonstrate that laser cooling, combined with  $V$ -scheme optical double-resonance spectroscopy, provides a sensitive means to measure isotope shifts and hyperfine splittings. Our technique is illustrated using the 398.8-nm  $(6s^2)^1S_0$ - $(6s6p)^1P_1$  and 555.6-nm  $(6s^2)^1S_0$ - $(6s6p)^3P_1$  transitions in a neutral ytterbium atomic beam having natural isotopic composition. With a precision comparable to existing approaches, our unique method has enabled the most complete single-technique survey to date of the  $^1S_0$ - $^1P_1$  isotope shifts and hyperfine splittings.

DOI: 10.1103/PhysRevA.63.023402

PACS number(s): 32.80.Pj, 95.30.Ky, 32.10.Fn

Merging laser cooling and high-resolution spectroscopy is rapidly becoming a powerful strategy for a variety of new spectroscopic experiments. The Doppler-free environment afforded by magneto-optical traps (MOT's) has, for example, recently enabled absorption measurements directly linking quantum interference to optical gain without population inversion in driven three-level  $V$ -scheme systems [1]. Additionally, the most accurate determination of *any* visible single photon atomic transition frequency [2] was recently realized using phase coherent measurements of the calcium  $^1S_0$ - $^3P_1$  transition in a  $^1S_0$ - $^1P_1$  MOT. Moreover, laser cooling has opened new avenues for hyperfine structure and linewidth measurements of one- and two-photon transitions in alkali metals [3].

$V$ -scheme optical double-resonance spectroscopy has been used to simplify complex molecular fluorescence and absorption spectra and explore state-changing inelastic molecular collisions [4]. In the simplest rendition of this technique, selective manipulation of ground-state populations with a pump laser and observations of modulated probe-induced fluorescence allows identification of transitions that share common ground states. We present an alternative formulation of this technique that utilizes a fixed frequency cooling laser on the pump transition to selectively depopulate *velocity classes* in an atomic beam. This enables, through weak probe fluorescence spectra from a *coupled transition*, measurements of the pump transition isotope shifts and hyperfine splittings. Specifically, longitudinal laser cooling is applied to an atomic beam composed of two or more isotopes whose Doppler-broadened resonance frequencies (Doppler profiles) overlap on the cooling transition. For a fixed laser frequency, this step generates *holes* in the velocity profiles of several isotopes (the atoms are decelerated) whose spectral locations are proportional to the pump transition isotope shifts and hyperfine splittings. These holes, and thus the pump transition frequency shifts, are measured by observing probe-induced fluorescence spectra from a coupled transition on which Doppler profiles for the different isotopes are well resolved. This novel approach eliminates the need for Doppler-free measurements inherent to other experimental methods [5–9].

Figure 1(a) depicts the two transitions used to demonstrate our technique. The 398.8-nm  $(6s^2)^1S_0$ - $(6s6p)^1P_1$  and 555.6-nm  $(6s^2)^1S_0$ - $(6s6p)^3P_1$  ytterbium (Yb) transi-

tions shown have enabled laser cooling of Yb atomic beams [10], magneto-optical trapping of single Yb isotopes [11–13], simultaneous trapping of Yb isotope pairs [14], new methods for probing the static and dynamic properties of magneto-optical traps [12], and are ideally suited to the experiment described here. Specifically, on the  $^1S_0$ - $^1P_1$  transition longitudinal atomic beam Doppler profiles for the various isotopes significantly overlap [see Fig. 1(b)] while on the  $^1S_0$ - $^3P_1$  transition these profiles are well resolved [see Fig. 1(c)]. Additionally, the  $^1S_0$ - $^3P_1$  isotope shifts and hyperfine splittings have been measured extensively [6] and Yb can be efficiently laser cooled using the  $^1S_0$ - $^1P_1$  transition. Significantly, these properties have allowed us to perform the most complete single-technique survey to date of the  $^1S_0$ - $^1P_1$  isotope shifts and hyperfine splittings and, in addition, to per-

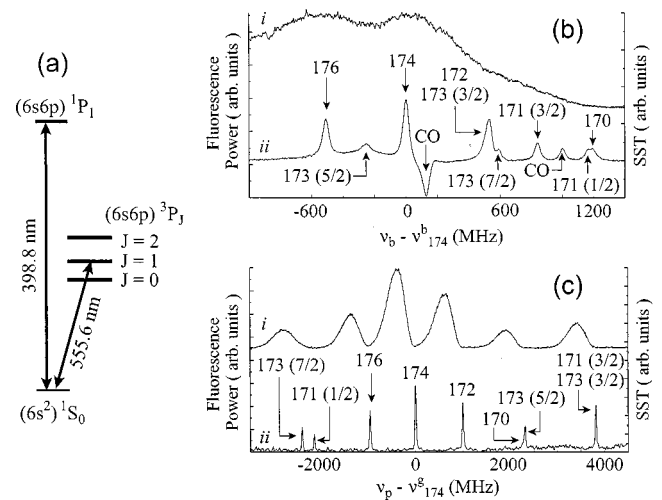


FIG. 1. (a) Partial Yb energy level diagram showing transitions relevant to the experiment. Note that the  $^1S_0$ - $^1P_1$  transition is not radiatively closed [11]. (b) Trace *i* (trace *ii*) is  $^1S_0$ - $^1P_1$  probe-induced atomic beam fluorescence (gas cell saturation spectra). (c) Trace *i* (trace *ii*) is  $^1S_0$ - $^3P_1$  probe-induced atomic beam fluorescence (gas cell saturation spectra).  $\nu_b$  ( $\nu_p$ ) 398.8-nm (555.6-nm) probe beam frequency; SST, saturation spectrometer transmission; CO, crossover resonance. Note that for (b) and (c), trace *i*, the probe lasers intersect the atomic beam at  $45^\circ$ . The inverted CO observed in (b) is due to optical pumping in the  $^{173}\text{Yb}$   $^1S_0$  ( $F=5/2$ ) ground state [15]. In (c), velocity profiles for a given isotope appear to the left of the corresponding Lamb dip.

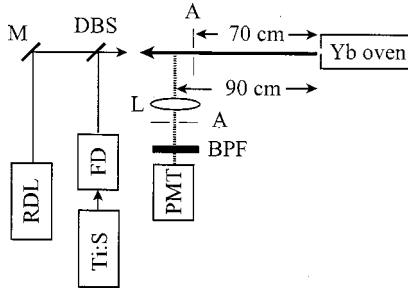


FIG. 2. Schematic diagram of the experiment. RDL, ring dye laser; Ti:S, Ti:sapphire laser; FD, resonant frequency doubler; M, mirror; DBS, dichroic beamsplitter; PMT, photomultiplier tube; BPF, bandpass filter; A, aperture; L, lens.

form the first spectral position measurement of the  $^{173}\text{Yb } ^1S_0(F=5/2) \rightarrow ^1P_1(F=7/2)$  transition.

The Yb atomic beam used for the experiment (see Fig. 2) is generated with an effusion oven (5-mm-diam nozzle) and collimated with a skimmer (6 mm diameter, located 70 cm from the nozzle). A single heater maintains the oven body and nozzle at 470 °C. Fluorescence from the observation region (1-cm<sup>2</sup> cross section, 90 cm downstream from the nozzle) is orthogonally imaged onto a photomultiplier tube (PMT) sampled by a digital oscilloscope (500- $\mu\text{s}$  overall system response time). A 555-nm bandpass filter ( $\sim 10$ -nm bandpass width) placed in front of the PMT allows selective detection of the 555.6-nm fluorescence. Vacuum levels during the experiment are  $< 10^{-8}$  Torr.

The collimated 398.8-nm cooling laser, generated by

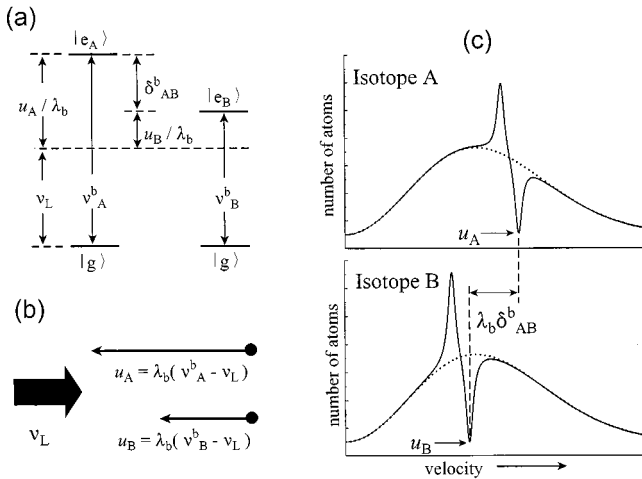


FIG. 3. (a) Simplified energy-level diagrams for two isotopes A and B whose cooling (pump) rest frame transition frequencies ( $\nu_A^b$  and  $\nu_B^b$ , respectively) are separated by a frequency shift  $\delta_{AB}^b = \nu_A^b - \nu_B^b$ .  $|g\rangle$ , ground state;  $|e_A\rangle$  ( $|e_B\rangle$ ), excited state for isotope A (B). (b) Due to overlapping Doppler-broadened resonance frequencies, A and B are simultaneously decelerated by a fixed-frequency cooling laser, frequency  $\nu_L$ . Here  $u_A = \lambda_b(\nu_A^b - \nu_L)$  [ $u_B = \lambda_b(\nu_B^b - \nu_L)$ ] is the initially resonant velocity class for isotope A [B] where  $\lambda_b = c/\nu_A^b \approx c/\nu_B^b$  is the wavelength of the cooling transition and the length of the arrows above  $u_A$  and  $u_B$  represent their relative magnitude. (c) Dashed (solid) lines are the velocity profiles for isotope A and B before (after) they traverse the slowing region.

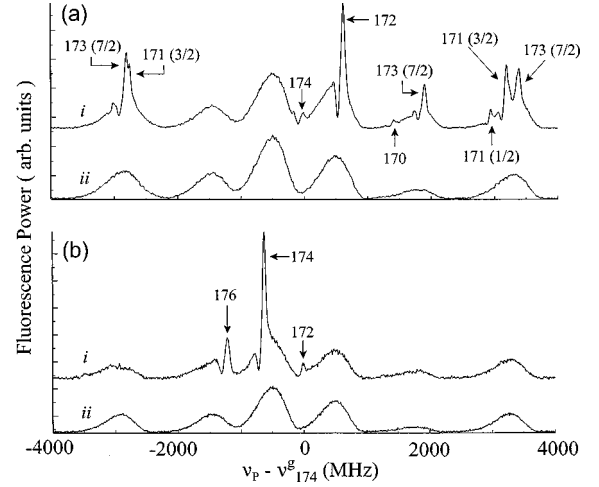


FIG. 4. Typical 555.6-nm fluorescence spectra observed for two different cooling laser detunings. For (a) [(b)],  $\Delta_L = \nu_{174}^b - \nu_L$ , is 130 MHz [1100 MHz] where  $\nu_{174}^b$  is the  $^{174}\text{Yb } ^1S_0 \rightarrow ^1P_1$  resonance frequency. In each, trace *i* (trace *ii*) is the spectra observed when the cooling laser is on (off).  $\nu_p$  ( $\nu_{174}^g$ ) is the probe ( $^{174}\text{Yb } ^1S_0 \rightarrow ^3P_1$  rest frame transition) frequency. Slowed-atom peaks are labeled by the corresponding isotope. For  $^{171}\text{Yb}$  and  $^{173}\text{Yb}$ , the numbers in parentheses are the total angular momentum quantum number  $F$  of the relevant  $^1P_1$  excited state.

resonantly frequency doubling the output of a Ti:sapphire (Ti:S) laser in an external buildup cavity (FD) has a  $1/e^2$  intensity diameter of 4 mm, contains 15 mW of power, and travels antiparallel to the atomic beam. The weak, collimated 555.6-nm probe beam is produced by a ring dye laser (RDL), has a  $1/e^2$  intensity diameter of 3 mm, and is adjusted, using a dichroic beam splitter (DBS), to nearly copropagate with the cooling laser. Separate saturation spectrometers provide frequency markers for the  $^1S_0 \rightarrow ^1P_1$  and  $^1S_0 \rightarrow ^3P_1$  transitions.

In Fig. 3(a), we depict simplified energy-level diagrams for two isotopes A and B, whose cooling (pump) transition rest frame frequencies ( $\nu_A^b$  and  $\nu_B^b$ , respectively) are separated by a frequency shift  $\delta_{AB}^b = \nu_A^b - \nu_B^b$ . Assuming overlapping longitudinal Doppler profiles, velocity class  $u_A = \lambda_b(\nu_A^b - \nu_L)$  [ $u_B = \lambda_b(\nu_B^b - \nu_L)$  for isotope B] will initially be resonant with, and hence slowed by, a fixed-frequency, counterpropagating cooling laser, where  $\nu_L$  is the cooling laser frequency,  $\lambda_b = c/\nu_A^b \approx c/\nu_B^b$  is the cooling transition wavelength,  $c$  is the speed of light, and  $\nu_L < \nu_B^b < \nu_A^b$  [see Fig. 3(b)]. Figure 3(c) depicts the resulting velocity distributions after the atoms have traversed the slowing region. Due to the slowing process, a hole at velocity  $u_A$  ( $u_B$ ) is generated in the velocity distribution for isotope A (B). These distributions are measured using probe-induced fluorescence spectra from a coupled transition, wavelength  $\lambda_g = c/\nu_A^g \approx c/\nu_B^g$ , where the velocity profiles are well resolved and the rest frame transition frequencies for A and B ( $\nu_A^g$  and  $\nu_B^g$ , respectively) are separated by a shift  $\delta_{AB}^g = \nu_A^g - \nu_B^g$ . Due to the depletion of atoms at  $u_A$  and  $u_B$ , dips will appear in the fluorescence profiles at frequencies  $\nu_A^d$  and  $\nu_B^d$ , respectively. Taking the frequency difference  $\Delta_{AB}^d = \nu_A^d - \nu_B^d$ ,

$$\Delta_{AB}^d = \delta_{AB}^g - (1/\lambda_g)(u_A - u_B) = \delta_{AB}^g - (\lambda_b/\lambda_g)\delta_{AB}^b. \quad (1)$$

TABLE I. Summary of the measured  $^1S_0-^1P_1$  isotope shifts and hyperfine splittings. For comparison, we include previously reported values.

Isotope	Shift relative to $^{174}\text{Yb}$ (MHz)			
	This work	Ref. [7]	Ref. [8]	Ref. [9]
168		1870.2(5.2)		
170	1175.7(8.1)	1172.5(5.7)	1195.0(10.8)	1158.9(8.1)
171 ( $F=1/2$ )	1151.4(5.6)	1136.2(5.8)		
171 ( $F=3/2$ )	832.5(5.6)	834.4(4.0)		
171 (centroid)	938.8(4.2)	935.0(3.3)	943.7(6.4)	923.4(3.0)
172	527.8(2.8)		530(4.0)	530.2(5.6)
173 ( $F=7/2$ )	578.1(5.8)			
174	0	0	0	0
176	-507.2(2.5)		-509.4(4.0)	-469.2(2.7)

Solving for  $\delta_{AB}^b$ ,

$$\delta_{AB}^b = (\lambda_g/\lambda_b)(\delta_{AB}^g - \Delta_{AB}^d). \quad (2)$$

Thus, varying  $\nu_L$ , measuring  $\Delta_{AB}^d$ , and using previously reported values for  $\delta_{AB}^g$  determines  $\delta_{AB}^b$  for two, or more generally, several isotopes. Note that for a significant range of cooling laser intensities, the width of the holes in the velocity distributions decreases as the cooling laser intensity decreases while the *hole visibility* (number of slowed atoms) does not [15,16]. Consequently, the precision with which  $\delta_{AB}$  is determined from single measurements of  $\Delta_{AB}^d$ , set in part by the hole width and visibility, *increases* as the cooling laser intensity decreases.

In Fig. 4(a) [Fig. 4(b)], we plot typical 555.6-nm fluorescence spectra observed when the 398.8-nm cooling laser detuning  $\Delta_L = \nu_{174}^b - \nu_L$  is 130 MHz [1100 MHz] where  $\nu_{174}^b$  is the  $^{174}\text{Yb}$   $^1S_0-^1P_1$  resonance frequency. In the figure,  $\nu_p$  [ $\nu_{174}^g$ ] is the probe [ $^{174}\text{Yb}$ ,  $^1S_0-^3P_1$  resonance] frequency. Trace *i* [trace *ii*] is 555.6-nm fluorescence spectra collected with the cooling laser on [off]. Scans are individually calibrated using observed  $^1S_0-^3P_1$  saturation spectra and the most accurate values available for the  $^1S_0-^3P_1$  isotope shifts and hyperfine splittings [6]. Slowed-atom peaks are labeled by the corresponding isotope. For  $^{171}\text{Yb}$  and  $^{173}\text{Yb}$  the total angular momentum quantum number  $F$  of the relevant  $^1P_1$  excited state is given in the parentheses. Note that for the  $^{171}\text{Yb}$  [ $^{173}\text{Yb}$ ]  $^1S_0$  ground state,  $F=1/2$  [ $F=5/2$ ]. In Fig. 4(a), simultaneous cooling of five isotopes is demonstrated and the  $^{171}\text{Yb}$   $F=1/2-3/2$  hyperfine splitting is observed directly. Additionally,  $^1S_0-^1P_1$  shifts and splittings that are difficult to resolve on this transition, for example,  $^{170}\text{Yb}$ - $^{171}\text{Yb}$  [ $F=1/2$ ] and  $^{172}\text{Yb}$ - $^{173}\text{Yb}$  [ $F=7/2$ ] [see Fig. 1(b)], are observed without the complication of overlapping emission or absorption profiles.

Several sources for error were considered when using these spectra to determine  $^1S_0-^1P_1$  isotope shifts and hyperfine splittings. The  $^1S_0-^3P_1$  shifts, having uncertainties of approximately 1 part in 1000 [6], produce error both through the absolute scan calibration and through their use in Eq. (2), contributing 1–4 MHz to our error budget. Asymmetries in

the observed velocity distribution holes, caused primarily by spectral proximity to slowed-atom peaks, limits the determination of  $\Delta_{AB}^d$  to  $\sim 5$  MHz or  $\sim 1/10$  of the full-width-at-half-maximum hole width observed here. Note this contribution to the error could potentially be reduced by using a lower-intensity cooling laser, a step that would reduce the hole width to  $\sim 20$  MHz [16]. Finally, nonlinearity of the probe laser scan contributes an error equal to a fixed percentage of the frequency separation between a given velocity distribution hole and the corresponding  $^1S_0-^3P_1$  saturation spectra feature. This percentage,  $\sim 0.6\%$ , was determined by directing the probe laser through a Fabry-Perot étalon and plotting the frequency marker position versus marker number as the probe laser was scanned.

Table I summarizes our measurements of the  $^1S_0-^1P_1$  isotope shifts and hyperfine splittings. Each value, given relative to the  $^{174}\text{Yb}$   $^1S_0-^1P_1$  rest frame resonance, is the average of 10–20 independent measurements. The ratio  $\lambda_g/\lambda_b$  was obtained using experimental values for the two transition wavelengths [17]. The centroid is defined as  $(\sum w_F)^{-1} \sum w_F \Delta \nu_F$  where  $w_F = (2F+1)$  and  $\Delta \nu_F$  is the splitting of the state with total angular momentum  $F$ . The uncertainties assigned to each value are standard deviations.

TABLE II. Magnetic dipole hyperfine interaction constant  $A_{171}$  for the  $^{171}\text{Yb}$   $^1P_1$  excited state derived from direct measurements of the  $^{171}\text{Yb}$   $^1S_0-^1P_1$  ( $F=1/2-3/2$ ) splitting. For comparison, we include previously reported values.

$A_{171}$ (MHz)	
This work	Previous work
-211.9(3.1)	-201.2(2.8) <sup>a</sup>
	-213.0(10) <sup>b</sup>
	-211.0(1.0) <sup>c</sup>
	-213.4(3.0) <sup>d</sup>
	-216.3(4.4) <sup>e</sup>

<sup>a</sup>Reference [7].

<sup>b</sup>Reference [18].

<sup>c</sup>Reference [19].

<sup>d</sup>Reference [8].

<sup>e</sup>Reference [20].

Note that the  $^1S_0\text{-}^1P_1$  isotope shift for  $^{168}\text{Yb}$  could not be measured in the present experiment due to the low natural isotopic abundance (0.13%) and spectral overlap between the  $^{168}\text{Yb}$ ,  $^{171}\text{Yb}$ , and  $^{173}\text{Yb}$   $^1S_0\text{-}^3P_1$  Doppler-broadened resonances. We find good agreement with the most recently published work [7,8] except for  $^{171}\text{Yb}$  ( $F=1/2$ ), which is larger than the value given in Ref. [7] by 0.7 standard uncertainties. Additional measurements are required to resolve this discrepancy, although we point out that Ref. [7] achieved higher frequency resolution (17 MHz compared to the  $\sim 50$ -MHz hole width observed here) and used a laser sideband technique that eliminates scan nonlinearity as a source of error.

Table II gives the magnetic dipole hyperfine interaction constant  $A_{171}$  for the  $^{171}\text{Yb}$   $^1P_1$  excited state extracted from direct measurements of the  $^{171}\text{Yb}$   $^1S_0\text{-}^1P_1$  ( $F=1/2\text{-}3/2$ ) splitting [see Fig. 3(a)]. With the exception of the anoma-

lously small value given by Ref. [7], there is good agreement between our result and those reported elsewhere [8,18–20].

Advances in studies of light-matter interactions and atomic structure can be expected as laser cooling continues to be incorporated into established high-resolution spectroscopic methods. We have presented a sensitive technique for measuring isotope shifts and hyperfine splittings that combines laser cooling and  $V$ -scheme optical double-resonance spectroscopy. This method has enabled, with an accuracy exceeding 1%, a nearly complete survey of the  $\text{Yb}$   $^1S_0\text{-}^1P_1$  isotope shifts and hyperfine splittings and is well suited to measurements of small frequency shifts.

The authors wish to thank C. Greiner and D. H. McIntyre for many helpful comments and suggestions. We gratefully acknowledge financial support from the National Science Foundation under Grant No. PHY-9870223.

- 
- [1] J. Kitching and L. Hollberg, *Phys. Rev. A* **59**, 4685 (1999).
- [2] H. Schnatz, B. Lipphardt, J. Helmcke, F. Riehle, and G. Zinner, *Phys. Rev. Lett.* **76**, 18 (1995); F. Riehle, H. Schnatz, B. Lipphardt, G. Zinner, T. Trebst, T. Binnewies, G. Wilpers, and J. Helmcke, in *Proceedings of the 1999 Joint Meeting of the European Frequency and Time Forum and the IEEE International Frequency Control Symposium, Braunschweig, Germany, 1999* (IEEE, Piscataway, 1999). The hydrogen  $1S\text{-}2S$  two-photon transition frequency has been measured with higher accuracy than the calcium  $^1S_0\text{-}^3P_1$  one-photon transition frequency. See M. Niering *et al.*, *Phys. Rev. Lett.* **84**, 5496 (2000).
- [3] M. Zhu, C. W. Oates, and J. L. Hall, *Opt. Lett.* **18**, 1186 (1993); R. W. Fox, S. L. Gilbert, L. Hollberg, J. H. Marquardt, and H. G. Robinson, *ibid.* **18**, 1456 (1993); A. G. Sinclair, B. D. McDonald, E. Riis, and G. Duxbury, *Opt. Commun.* **106**, 207 (1994); N. Ph. Georgiades, E. S. Polzik, and H. J. Kimble, *Opt. Lett.* **19**, 1474 (1994); C. W. Oates, K. R. Vogel and J. L. Hall, *Phys. Rev. Lett.* **76**, 2866 (1996).
- [4] M. E. Kaminsky, R. T. Hawkins, F. V. Kowalski, and A. L. Schawlow, *Phys. Rev. Lett.* **36**, 671 (1976); R. Teets, R. Feinberg, T. W. Hänsch, and A. L. Schawlow, *ibid.* **37**, 683 (1976); W. Demtröder, D. Eisel, H. J. Foth, G. Höning, M. Raab, H. J. Vedder, and D. Zevgolis, *J. Mol. Struct.* **59**, 291 (1980); M. A. Johnson, C. R. Webster, and R. N. Zare, *J. Chem. Phys.* **75**, 5575 (1981); F. Bylicki, G. Persch, E. Mehdizadeh, and W. Demtröder, *Chem. Phys.* **135**, 255 (1989).
- [5] M. D. Levenson, *Introduction to Nonlinear Laser Spectroscopy*, 1st ed. (Academic Press, New York, 1982).
- [6] W. A. van Wijngaarder and J. Li, *J. Opt. Soc. Am. B* **11**, 2163 (1994).
- [7] K. Deilamian, J. D. Gillaspay, and D. E. Kelleher, *J. Opt. Soc. Am. B* **10**, 789 (1993).
- [8] P. Grundevik, M. Gustavsson, A. Rosén, and S. Svanberg, *Z. Phys. A* **283**, 127 (1977); P. Grundevik, M. Gustavsson, A. Rosén, and S. Rydberg, *ibid.* **292**, 307 (1979).
- [9] Y. Chaiko, *Opt. Spectrosc.* **18**, 200 (1965); **20**, 424 (1966).
- [10] M. Watanabe, R. Ohmukai, U. Tanaka, K. Hayasaka, H. Imajo, and S. Urabe, *J. Opt. Soc. Am. B* **11**, 2377 (1996); R. Ohmukai, H. Imajo, K. Hayasaka, U. Tanaka, M. Watanabe, and S. Urabe, *Appl. Phys. B: Lasers Opt.* **64**, 547 (1997).
- [11] T. Loftus, J. R. Bochinski, R. Shivitz, and T. W. Mossberg, *Phys. Rev. A* **61**, 051401(R) (2000).
- [12] T. Loftus, J. R. Bochinski, and T. W. Mossberg, *Phys. Rev. A* **61**, 061401(R) (2000).
- [13] K. Honda, Y. Takahashi, T. Kuwamoto, M. Fujimoto, K. Toyoda, K. Ishikawa, and T. Yabuzaki, *Phys. Rev. A* **59**, R934 (1999); T. Kuwamoto, K. Honda, Y. Takahashi, and T. Yabuzaki, *ibid.* **60**, R745 (1999).
- [14] T. Loftus, J. R. Bochinski, and T. W. Mossberg, *Phys. Rev. A* (to be published).
- [15] D. H. McIntyre (private communication).
- [16] N. Beverini, F. Giammanco, E. Maccioni, F. Strumia, and G. Vissani, *J. Opt. Soc. Am. B* **6**, 2188 (1989); T. Loftus (unpublished).
- [17] W. C. Martin, R. Zalubas, and L. Hagan, *Atomic Energy Levels—The Rare Earth Elements*, Natl. Bu. Stand. (U.S.) Circ. No. NSRDS-NBS 60 (U.S. GPO, Washington, D.C., 1978).
- [18] R. W. Berends and L. Maleki, *J. Opt. Soc. Am. B* **9**, 332 (1992).
- [19] H. Liening, *Z. Phys. A* **320**, 363 (1985).
- [20] B. Budick and J. Snir, *Phys. Rev.* **178**, 18 (1969).